minerals

MDPI

Article

Volcano–Sedimentary Processes on an Ancient Oceanic Seafloor: Insights from the Gimigliano Metaophiolite Succession (Calabria, Southern Italy)

Federica Barilaro [1,2,*], Andrea Di Capua [2,*], Giuseppe Cianflone [1,3], Giovanni Turano [1], Gianluca Robertelli [1], Fabrizio Brutto [1], Giuseppe Ciccone [1], Alessandro Foti [1], Vincenzo Festa [4] and Rocco Dominici [1,3]

[1] Department of Biology, Ecology and Earth Science, University of Calabria, 87036 Arcavacata di Rende, Italy
[2] CNR—Institute of Environmental Geology and Geoengineering, Via R. Cozzi 53, 20125 Milan, Italy
[3] E3 (Earth, Environment, Engineering) Spin-Off, University of Calabria, Via Ponte Bucci, Cubo 15B, 87036 Rende, Italy
[4] Earth Sciences and Geo-Environmental Department, University of Bari Aldo Moro, Via E. Orabona, 4, 70125 Bari, Italy
* Correspondence: federica.barilaro@unical.it (F.B.); andrea.dicapua@igag.cnr.it (A.D.C.)

Abstract: This study investigates the volcano–sedimentary processes that occurred in an oceanic branch of the Western Tethys, now part of the Gimigliano–Monte-Reventino metaophiolite Unit, exposed at the southeastern termination of the Sila Piccola Massif, within the northern sector of the Calabria–Peloritani terrane (Calabria, southern Italy). Fieldwork, petrography, and mineralogical analyses on the Gimigliano metaophiolite succession have identified five distinct volcano–sedimentary lithofacies. These lithofacies are characterized by mineral assemblages of epidote, chlorite, quartz, and albite, with minor amounts of muscovite and calcite, resulting from high-pressure–low-temperature (HP-LT) metamorphism followed by low-grade greenschist metamorphism of mid-oceanic ridge basalt (MORB)-type volcanic products. Based on their stratigraphic and textural features, these lithofacies have been interpreted as metabasaltic flow layers emplaced during effusive volcanic eruptions and metahyaloclastic and metavolcaniclastic deposits formed by explosion-driven processes. This lithofacies assemblage suggests that the Gimigliano area likely represented an oceanic sector with high rates of magmatic outflows, where interactions between magma and water facilitated explosive activity and the dispersion of primary volcaniclastic deposits, mainly from the water column, in addition to the emplacement of basaltic lava flow. In contrast, other metaophiolite complexes in the Calabria region, characterized by the presence of pillow basalts, were areas with low effusive rates. The coexistence of these differences, along with the extensive presence of metaultramafites, portrays the Calabrian branch of the Tethys as a slow-spreading oceanic ridge where variations in surficial volcanic processes were controlled by differences in the effusion rates across its structure. This study is a valuable example of how a volcano–sedimentary approach to reconstructing the emplacement mechanisms of metaophiolite successions can provide geodynamic insights into ancient oceanic ridges.

Keywords: metaophiolites; greenschists; lava flows; primary volcaniclastic deposits; Western Tethys; slow-spreading oceanic ridge

check for updates

Academic Editors: Federica Zaccarini and Urs Klötzli

Received: 19 March 2025
Revised: 8 May 2025
Accepted: 20 May 2025
Published: 22 May 2025

Citation: Barilaro, F.; Di Capua, A.; Cianflone, G.; Turano, G.; Robertelli, G.; Brutto, F.; Ciccone, G.; Foti, A.; Festa, V.; Dominici, R. Volcano–Sedimentary Processes on an Ancient Oceanic Seafloor: Insights from the Gimigliano Metaophiolite Succession (Calabria, Southern Italy). *Minerals* **2025**, *15*, 552. https://doi.org/10.3390/min15060552

Copyright: © 2025 by the authors. Licensee MDPI, Basel, Switzerland. This article is an open access article distributed under the terms and conditions of the Creative Commons Attribution (CC BY) license (https://creativecommons.org/licenses/by/4.0/).

1. Introduction

Ongoing advances in the study of oceanic environments have frequently demonstrated that effusive processes account for only a portion of the volcanic activity associated with

deep-sea eruptive processes (e.g., [1,2]). Thick accumulations of primary volcaniclastic layers (sensu [3]) are, in fact, widely observable worldwide along oceanic ridges (e.g., [1,4–7]). It is worth noting that different types of effusive and explosive products, as well as their volumetric occurrence and distribution across an oceanic ridge, are also observed to be correlated with spatial variability and magmatological behavior of eruptive regions and/or with the deep geodynamic setting of the ridge itself (e.g., [7–9]). It derives that the study of ancient volcano–sedimentary sequences in ophiolitic contexts is crucial for reconstructing the evolution of ancient oceanic realms and for a better constraint on the evolution of geodynamic processes leading to the generation of oceanic seafloor through geological time. The Tethys Ocean arguably represents the most extensively studied example of ancient oceanic seafloor (e.g., [10,11]), as its generation, evolution, and disruption along various convergent margins have played, and continue to play, a fundamental role in shaping the geodynamic processes underlying the evolution of Earth's plate tectonic regime since the early Mesozoic (e.g., [12,13]). Nevertheless, accuracy in the recognition of volcano–sedimentary facies and the related mechanisms that drove the evolution of its sedimentary systems is often hard to gain, especially in areas where ophiolite successions underwent metamorphism and deformation due to subduction-related processes. Therefore, reconstructions of Tethyan geodynamics in different areas suffer from the paucity of solid volcano-stratigraphic models, and this limits the possibility of better identification of ancient magmatic plumbing systems, ridge morphologies, and oceanic spreading rates.

In this scientific framework, the present work aims to explore the emplacement mechanisms of volcano–sedimentary products associated with the Jurassic Tethyan branch of Calabria (southern Italy—Figure 1) [14,15]. Integrated field observations, combined with petrographic and mineralogical analyses of metabasites belonging to the metaophiolite succession of Gimigliano (southeastern termination of the Sila Piccola Massif—Figure 1), have led to the identification of several lithofacies, with the main objective of reconstructing the nature of the volcano–sedimentary protoliths and the processes responsible for their generation and emplacement. Furthermore, comparison with the literature data on other volcano–sedimentary successions in the Calabria region [14,15] has revealed key similarities and differences, enhancing our understanding of the magmatic processes that governed the evolution of this branch of the Tethyan Ocean. By comparing fossil analogues in Calabria with modern oceanic ridge successions worldwide, it has been possible to gain insights into the ancient ridge morphology and magmatological behavior of the Calabrian ridge.

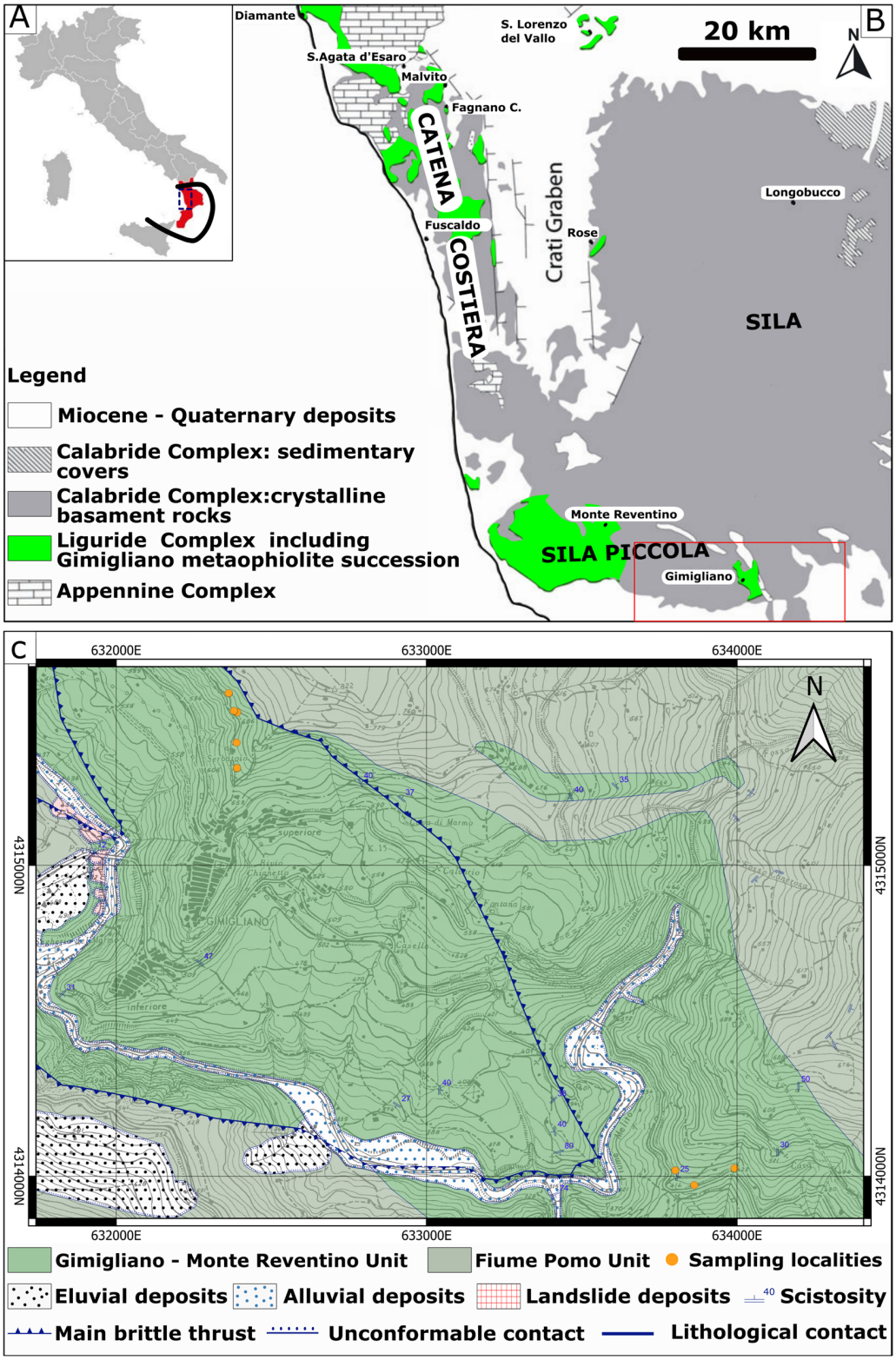

Figure 1. Geological setting of the Gimigliano metabasite succession. (**A**) Location of the Calabria region (in red) within the Italian territory, and outline of the Calabria–Peloritani terrane indicated by the black line. Dotted square indicates area of Figure 1B. (**B**) Simplified geological map of the Sila Massif in the framework of the north-western part of Calabria–Peloritani terrane, redrawn from [16] and [17]. The red rectangle indicates the area object of the CARG (Geological CARtography) Project—Geologic and Geothematic cartography, sheet n. 575 "Catanzaro". (**C**) Detail of the geological map of the Gimigliano area showing the sampling localities. Coordinates are in WGS84—UTM 33N.

2. Geological Setting

The study area is in the municipality of Gimigliano (Calabria, southern Italy) at the southeastern termination of the Sila Piccola Massif, within the northern sector of the Calabria–Peloritani terrane (Figure 1). The Calabria–Peloritani terrane [18] is a complex, arcuate segment of the peri-Mediterranean Alpine nappe system, which links the Apennine thrust-and-fold belts of southern Italy with the Maghrebian chain in Sicily [14,18,19]. It is primarily composed of crystalline basement rocks resulting from a polyorogenic, multi-stage history that began during the Variscan orogenesis and culminated in the Alpine metamorphic cycle (e.g., [20–23]). Although less extensive, oceanic-derived units—dating back to the Jurassic–Cretaceous and interpreted as remnants of the Tethys Ocean, which once separated the African and European plates [15,24–30]—are confined to the northern sector of the Calabria–Peloritani terrane, where they outcrop discontinuously (e.g., [15,20,31]). These units, referred to as the Liguride Complex by [32], are believed to have initially been involved in subduction processes and were later progressively deformed and accreted during Europe-verging continent–continent collision events ([19] and references therein). The Liguride Complex represents the intermediate unit among the three main tectono–stratigraphic complexes of the northern Calabria–Peloritani terrane, each composed of distinct tectono-metamorphic units [14,19,26,33–35]. It is, in fact, covered by the Calabride Complex, which includes late-Hercynian continental crust, locally with Meso–Cenozoic sedimentary or weakly metamorphosed cover [35,36], and lies above the complex of Apennine units. The oceanic-derived units, initially classified by [14] into four separate groups—Diamante–Terranova, Malvito, Gimigliano–Mt-Reventino, and Malvito Units—were later consolidated by [15] due to their similar tectono-metamorphic evolution. The oceanic-derived sequence includes mantle-derived ultramafic rocks, represented by serpentinized peridotites from a lherzolitic–harzburgitic protolith with typical geochemical signatures of oceanic peridotites, often found in association with ophicalcites and exposed only in the Gimigliano and Monte Reventino area [30,37–39]. This oceanic basement also includes massive and foliated metabasites (e.g., [14,30,37]). Geochemical and petrological investigations indicate that these metabasites are derived from subalkaline transitional mid-ocean ridge basalts (T-MORB type) with a tholeiitic affinity (e.g., [15,29,30]). Locally, well-preserved pillow structures, along with rare associated Mg-gabbros, metabreccias, and metahyaloclastites, have been observed ([14,31,35] and ref. therein). Porphyritic and aphyric pillow lavas have been reported in the Malvito, S. Agata di Esaro, and Rose areas [14,30,31], while the Diamante–Terranova metabasites, which contain glaucophane, include highly deformed porphyritic pillows, pillow breccias, and massive fine-grained mafic rocks in the San Lorenzo del Vallo outcrops [30]. The complex sedimentary cover of the ophiolitic succession is composed of pelagic components, such as metaradiolarites and Calpionella meta-limestones dating from the Tithonian–Neocomian age ([40,41]), as well as flyschoid facies, which include metapelites, metarenites, and metalimestones of indeterminate age ([42] and references therein), interpreted as deposits of proximal terrigenous origin [43]. The Gimigliano–Monte-Reventino Unit, exposed in a tectonic window at Gimigliano, represents the lowermost structural unit of the nappe stack in the study area ([44,45]). Previous studies indicate that this unit is composed of serpentinites, metabasalts, metagabbros, and metadoleritic dykes with marbles, quartzites, phyllitic quartzites, and calcschists representing the metamorphic products of the original sedimentary cover of the oceanic crust [16,30,38,42]. The ophiolitic sequence underwent high-pressure–low-temperature (HP-LT) metamorphism followed by retrogression under greenschist facies conditions (e.g., [15]). The age of the Gimigliano–Monte-Reventino Unit remains uncertain. Amodio-Morelli et al. [14] propose a Late-Jurassic–Cretaceous age, whereas Colonna and Zanettin Lorenzoni [46], relying on paleontological data, advocate for a Ladinian–Carnian age. In contrast, Vai [47]

correlates the basic volcanics of the Gimigliano area with the magmatic events in the southern Alps and Dinarides, pointing to a Middle Triassic origin.

3. Materials and Methods

This study results from a comprehensive analysis of the literature data, geological surveys, and stratigraphic reconstruction of the Gimigliano metaophiolite succession. The geological survey of the Gimigliano area was conducted on a 1:10,000 topographic map (Cassa per il Mezzogiorno, 1958) within the framework of the CARG (Geological CARtography) Project—Geologic and Geothematic cartography, sheet n. 575 "Catanzaro". This project enabled the sampling of composite stratigraphic logs from the Gimigliano metaophiolite succession during the last semester of 2024, providing key data for this study on the Gimigliano greenschist member (here referred to as Gimigliano metabasite succession), which outcrops in the territories of the Gimigliano municipality and Cavorà village. The samples were processed and analyzed at the Department of Biology, Ecology, and Earth Sciences, University of Calabria. Twenty samples were embedded in resin and thin-sectioned to approximately 30 µm (28 × 48 mm) to facilitate detailed petrographic analysis. These thin sections were analyzed for microfacies characterization using standard petrographic techniques with an OPTIKA polarizing optical microscope equipped with an OPTIKA digital camera. Bulk mineral composition was assessed through X-ray diffraction (XRD) analysis using a Panalytical Xpert Pro PW 3040/60 system, with scans collected in the 2°–62° 2θ range, a step size of 0.02°, and a counting time of 1 s per step.

Petrographic and mineralogical analysis results, along with geological fieldwork data, were integrated to refine the characterization of the Gimigliano metabasite succession. It was compared with regional geological models to enhance the understanding of the stratigraphy and emplacement mechanisms.

4. Results

The Gimigliano–Monte-Reventino Unit is exposed in the Gimigliano area, with thicknesses exceeding 300 m. However, its full thickness is challenging to determine due to its complex deformation history, which includes ductile/brittle folding and thrusting. The lower part of this metaophiolite assemblage predominantly comprises peridotite and serpentinite, displaying colors ranging from intense green to greenish-black (Figure 2A), with common associated ophicalcite rocks (Figure 2B). Above this layer, well-foliated to massive greenschist rocks of the metabasite succession occur (Figure 2C). This intermediate part is significantly thicker than the underlying metaultramafic rocks and is the primary focus of the present study. On top, the unit is capped with a metasedimentary succession that includes schists, metaolistostrome bodies, metarenites, calceschists, and phyllites (Figure 2D,E).

Despite the discontinuous and fragmentary nature of the outcrops, a stratigraphic analysis of the succession has been conducted. Five main metabasite lithofacies (Table 1 and Figure 2F) have been identified and hereafter described, with the abbreviations used in the related figures following [48]. For detailed information on the geochemistry and petrology of Gimigliano metabasite succession, please refer to [15,29,30,35,38].

4.1. Lithofacies A

Lithofacies A crops out in the lower and central part of the succession (Figure 2F), rarely in the uppermost part, and has a cumulative thickness of more than 300 cm. It displays a foliated texture characterized by well-defined, laterally continuous, and subparallel main layering (Figure 3A). The dominant color is a greenish hue, interspersed with lighter yellowish-green and darker green centimeter-thick bands. Minor, millimeter-thick

reddish-brown bands, irregular in shape, are occasionally present within the foliation, subtly alternating with the dominant greenish-gray matrix. The rock has a fine-grained, laminated texture with visible foliation planes that are slightly undulating. Layering varies from widely spaced to closely spaced. Both more compact and massive domains, as well as portions appearing slightly more porous, are observed. Micropores, elongated along the foliation, occur. This lithofacies is organized into laterally continuous and vertically alternating sub-horizontal units on a metric scale. XRD analysis reveals that cristobalite, clinozoisite, albite, and chlorite are the main components of Lithofacies A.

Table 1. Main characteristics of Gimigliano metabasite lithofacies.

Lithofacies	Macroscopic Features	Microscopic Features	Main Minerals	Interpretation (Putative Eruptive Process)
A	Fine-grained, laminated, greenish with yellowish-green and darker green bands, minor reddish-brown bands	Well-developed foliation, quartz–albite–epidote porphyroblasts, micropores elongated along foliation	Cristobalite, clinozoisite, albite, chlorite	Fallout deposits through water column
B	Fine- to medium-grained, massive to weakly foliated, green (dark to light) with bluish tints and whitish speckles	Lepido-nematoblastic texture, epidote and hornblende crystals wrapped by foliation	Clinozoisite, albite, clinochlore, lawsonite	Sheet basalts
C	Well-foliated, greenish with brownish-violet and whitish domains, alternating fine- and coarse-grained layers	Grano-lepido-nematoblastic texture, epidote and chlorite aggregates, quartz–albite–epidote layers	Clinochlore, epidote, albite, quartz, muscovite	Sheet hyaloclastites
D	Fine- to medium-grained, compact, intense green with silvery sheen, soapy feel	Alternating mafic and felsic layers, pseudofelty muscovite structures, epidote trains	Muscovite, quartz, albite, ferronian clinochlore, epidote	Alternation of flow and fall deposits, hyaloclastic in composition
E	Fine- to medium-grained, compact, dark green with bluish-black tones and silvery reflection	Alternating chlorite- and quartz–calcite-dominated bands, epidote and rare amphibole porphyroblasts	Chlorite, quartz, calcite, epidote, muscovite, albite	Hybrid facies with larger amounts of sedimentary particles

Based on microscopic observations, this lithofacies is very fine-grained, with a well-developed foliation determined by the segregation of dark and light sub-horizontal layers. The dark regions are mainly composed of chlorite–epidote, whereas light areas are composed of quartz–albite and epidote in small porphyroblasts (Figure 3B), constituted by the alignment of flattened or elongated elements of quartz, albite, or quartz + epidote (Figure 3C). In addition, laterally discontinuous submillimeter-thick lenses of quartz + epidote + minor albite are intercalated within the main foliation (Figure 3D).

Macro- and microscale observations suggest that Lithofacies A includes volcanogenic deposits (sensu [49]), in which the alternation of mafic and felsic bands is due to primary mechanisms of suspension settling.

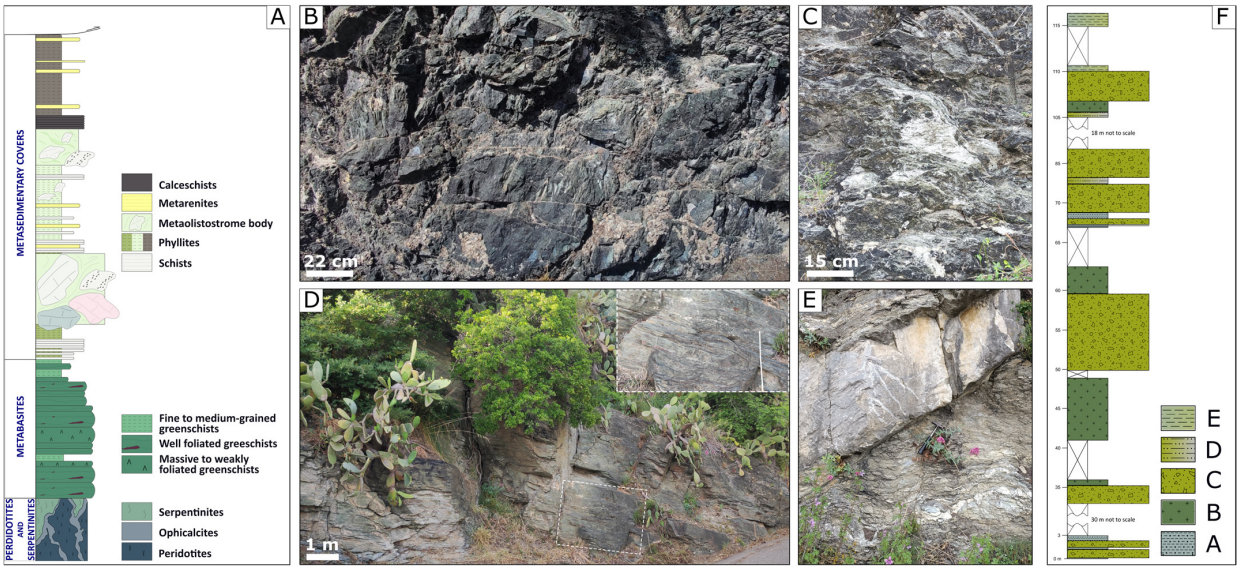

Figure 2. Main lithological features of the Gimigliano ophiolite succession. (**A**) Representative composite log of the Gimigliano ophiolite succession measured in the Gimigliano area (not to scale). (**B**) Metaultramafic rocks formed of serpentinites. (**C**) Ophicalcites found in closed association with serpentinite showing a brecciated fabric. (**D**) Metabasite layers characterized by a strong foliation. Image bounded by white dotted line in the upper right corner shows foliation details. (**E**) Marble olistolith in a strongly foliated metapelite to metarenite bed. (**F**) Detailed representative log of the Gimigliano metabasites. Letters correspond to the lithofacies of Table 1. The scale is in meters.

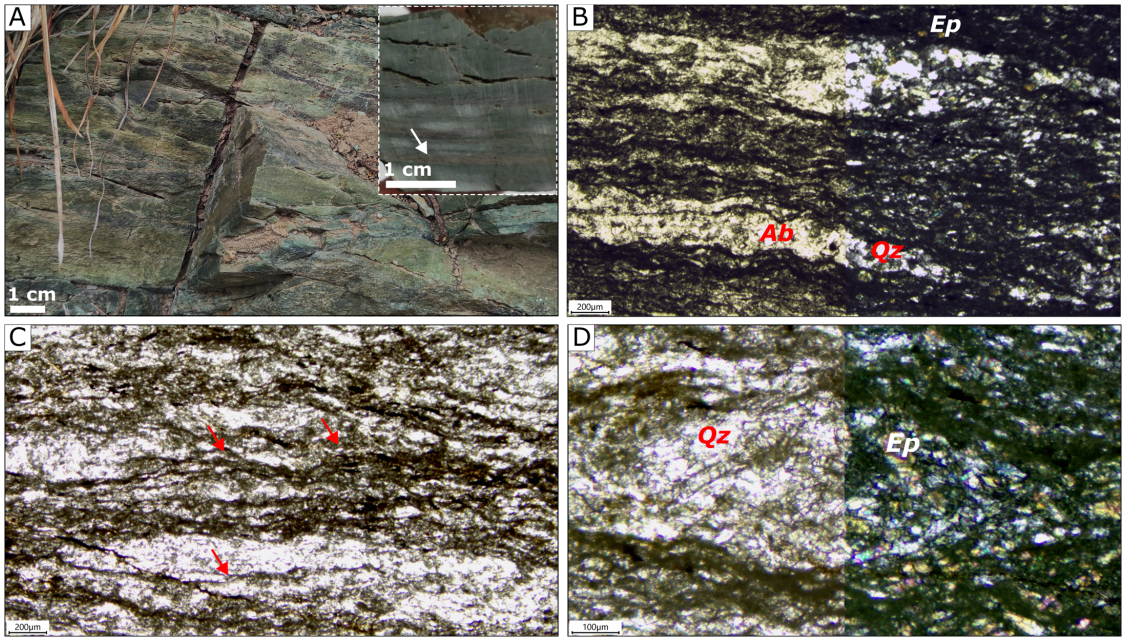

Figure 3. Lithofacies A. (**A**) Field image showing a well-developed foliation defined by continuous, slightly undulating, parallel layers with green hue, interspersed with yellowish-green and dark bands along with occasional reddish-brown irregular laminae (white arrow). (**B**) Thin-section photomicrograph of alternating dark and light sub-horizontal layers. Dark layers are fine-grained and dominated by chlorite and epidote (Ep—often as porphyroblasts); light layers are coarser and dominated by quartz (Qz) and albite (Ab). Plane (**left**) and crossed (**right**) polarized light. (**C**) Thin-section photomicrograph showing flattened elements of quartz and albite (red arrows) aligned along the foliation. Plane polarized light. (**D**) Thin-section photomicrograph showing a discontinuous lens composed of quartz, epidote, and albite wrapped by the foliation. Plane (**left**) and crossed (**right**) polarized light.

4.2. Lithofacies B

Lithofacies B dominates the central part of the succession, with a cumulative thickness of ca. 600 cm (Figure 2F). It displays a compact, massive to weakly foliated texture (Figure 4A). The dominant color is green, ranging from dark green to lighter greenish hues, with some portions exhibiting a slight sheen. Bluish tonalities, along with whitish speckles and streaks, are also present. The texture is fine- to medium-grained, with the main foliation defined by the preferred orientation of platy/tabular minerals. Blackish amphiboles are particularly noticeable to the naked eye, standing out clearly against the finer-grained matrix. The layering is fine and closely spaced, though not very pronounced. Porosity is generally absent or barely visible. This lithofacies typically occurs in tabular layers, ranging from several centimeters to several decimeters in thickness. Mineralogically, it contains clinozoisite, albite, clinochlore, and lawsonite, as indicated by XRD analysis.

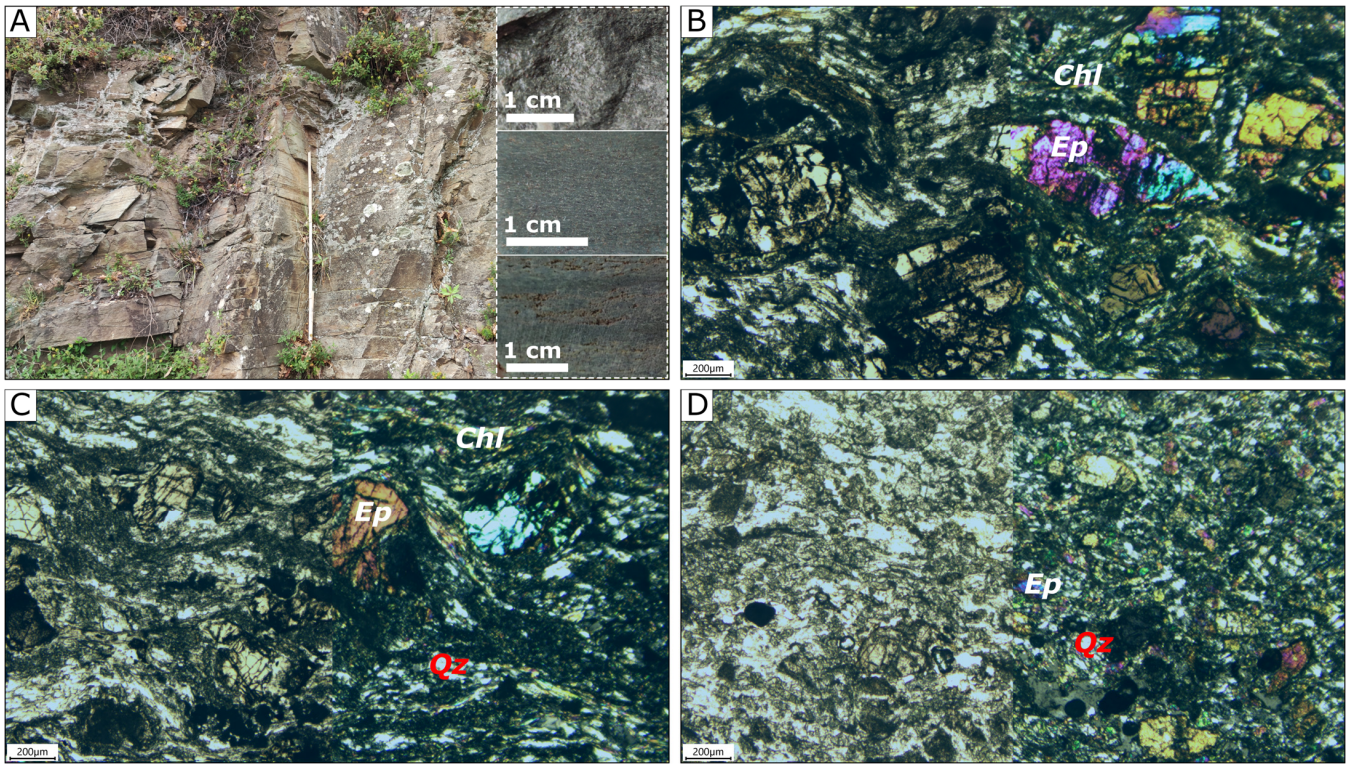

Figure 4. Lithofacies B. (**A**) Field image of tabular layers characterized by a compact, massive (upper and middle close-up view) to lightly foliated texture (lower close-up view), featuring green hues, bluish tints, and whitish speckles. (**B**) Thin-section photomicrograph characterized by a lepido-nematoblastic dominated by chlorite wrapping porphyroblasts of epidote (Ep). Plane (**left**) and crossed (**right**) polarized light. (**C**) Thin-section photomicrograph characterized by a lepido-nematoblastic texture of chlorite (Chl), quartz (Qz), and plagioclase with porphyroblasts of epidote (Ep). Plane (**left**) and crossed (**right**) polarized light. (**D**) Thin-section photomicrograph showing a fine-grained groundmass composed of quartz and plagioclase, with minor chlorite, embedding porphyroblasts of epidote (Ep). Plane (**left**) and crossed (**right**) polarized light.

Microscopic observations show a lepido-nematoblastic texture characterized by crystals of epidote, hornblende, and minor plagioclase wrapped around by the foliation, which is alternatively dominated by chlorite and lawsonite, with very fine-grained quartz and plagioclase (Figure 4B,C), or by quartz and plagioclase (Figure 4D).

This massive lithofacies is interpreted as submarine tabular basaltic layers.

4.3. Lithofacies C

Lithofacies C is the most representative facies, predominantly occurring at the bottom and on top of the succession (Figure 2F), with a cumulative thickness exceeding 3000 cm. It consists of greenish foliated rocks, interspersed with brownish-violet and whitish domains (Figure 5A). It is characterized by a well-developed foliation at a millimetric to centimetric scale, featuring alternating fine-grained light green to pale yellow layers and coarser, dark green, laterally discontinuous, and bright regions in a very fine-grained matrix (Figure 5B). The overall structure reveals portions of tightly spaced banding and others where the separation between the layers is wider. Layering varies from undulating to laterally discontinuous. Sub-rounded to rounded particles, typically millimetric in size and ranging from whitish to yellowish (Figure 5C), as well as reddish fragments varying from centimetric to pluri-centimetric in size (Figure 5D), are embedded within the main foliation and occasionally form laterally continuous layers. Flattened whitish porous and laterally discontinuous laminae locally disrupt the stratification of greenish-toned layers. XRD analyses indicate that clinochlore, epidote, albite, quartz, and muscovite represent the main mineralogical phases in variable amounts.

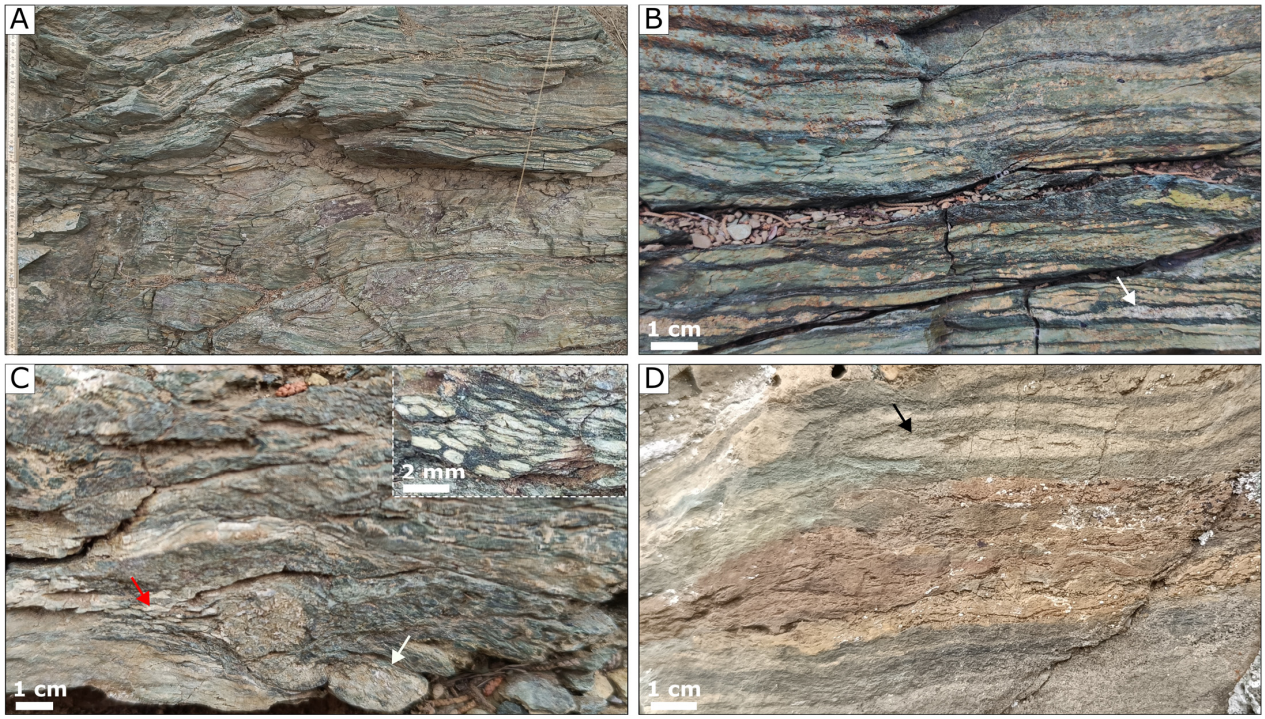

Figure 5. Field appearance of Lithofacies C. (**A**) Strongly foliated greenschist outcrop that characterized Lithofacies C. (**B**) A close up view of outcrop in (**A**), featuring alternations of fine-grained light green to pale yellow layers with coarser, bright, dark green bands. White arrow points to a white, discontinuous, flattened lamina. (**C**) Discontinuous dark green, bright, coarse region containing rounded centimetric-scale fragments (white arrow) and whitish to yellow, millimetric-scale sub-rounded to rounded, flattened particles (red arrow). The enlarged view shows these sub-rounded to rounded fragments from whitish to yellow in a dark green groundmass. (**D**) A detailed view of a reddish fragment intercalated within the foliation. Note also the presence of whitish, flattened, and discontinuous layers (black arrow).

Petrographic observations reveal a complex grano-lepido-nematoblastic texture, reflecting the alternations of laterally continuous and discontinuous layering with different mineralogical assemblage at mesoscale observations. Dark green laminae consist of very fine, dark brown, chlorite-dominated groundmass with dispersed porphyroblasts and/or

aggregates of epidote minerals, aggregated of epidote, albite, and quartz, or, rarely, coarse-grained, dark brown, fragmented particles (Figure 6A). When they are bright, dark green laminae correspond to bands of coarse-grained epidote crystals (Figure 6B). Pale yellow to light green laminae and fragments are composed of fine-grained albite-quartz dominated layers, with a variable amount of epidote, or quartz–albite–epidote layers. When they are arranged in laterally continuous laminae, they show a well-developed foliation, underlined by dark brown to black, very fine bands that can either be continuous or discontinuous. White porous laminae display a quartz-dominated groundmass with minor chlorite, containing porphyroclasts of albite and rare amphiboles, as well as porphyroblasts of epidote (Figure 6C). Sometimes, these porous layers show a variolitic texture of divergent acicular crystals of albite (Figure 6D). Finally, reddish to brown fragments show alternations of fine-grained, epidote–chlorite- and quartz–albite-dominated layers concentrically distributed from their core (Figure 6E). Rare pyroxenes, totally transformed into epidote after metamorphism, are embedded in the fine-grained groundmass (Figure 6E). Locally, small dark portions composed of a very fine-grained groundmass of microcrystalline calcite and rare phenocrystals of epidote are recognized (Figure 6F).

Macro- and microscale observations suggest that the protoliths of Lithofacies C are hyaloclastic deposits, predominantly accumulated through massive individual flows.

4.4. Lithofacies D

Lithofacies D occurs in the uppermost part of the studied succession (Figure 2F) with a cumulative thickness of ca. 150 cm. It consists of a fine- to medium-grained, compact, and well-foliated rock, characterized by an intense green color with variations from dark green to greenish-gray tonalities (Figure 7A). It displays a distinct silvery luster, with a silky sheen, particularly evident along the schistosity planes, and a soapy feel on the foliation surface. The grain size varies, with a predominantly fine-grained matrix transitioning to coarser zones, where larger, generally lamellar mineral crystals are visible. The foliation is well developed, with alternating lighter and darker bands, typically forming tight layering from parallel to undulating layers. However, in some areas, the texture appears more massive, partially obscuring the schistosity. Minor clasts and particles of slightly different composition and whitish color, ranging from millimetric to a few centimeters in size, are wrapped into the foliation. Qualitative XRD analyses reveal a mineralogical assemblage of muscovite, quartz, albite, ferronian clinochlore, and epidote.

Petrographic observations show alternations of fine-grained mafic layers, composed of epidote and chlorite, and felsic layers, constituted of quartz and albite (Figure 7B). Locally, the presence of pseudofelty structures of muscovite, permeating the groundmass (Figure 7C) or wrapping coarser crystals (Figure 7D), characterizes the layers. Chlorite bands with well-developed foliation are typical of silvery luster layers (Figure 7E) and include single crystals or trains of epidote (Figure 7F). Clastic fragments, recognized at the mesoscale, are composed of a fine-grained quartz + epidote + calcite mineralogical assemblage under microscopic observations.

Lithological and microscale features of Lithofacies D indicate primary volcaniclastic layers settled down by the alternation of low concentrated flows with their plumes as protoliths.

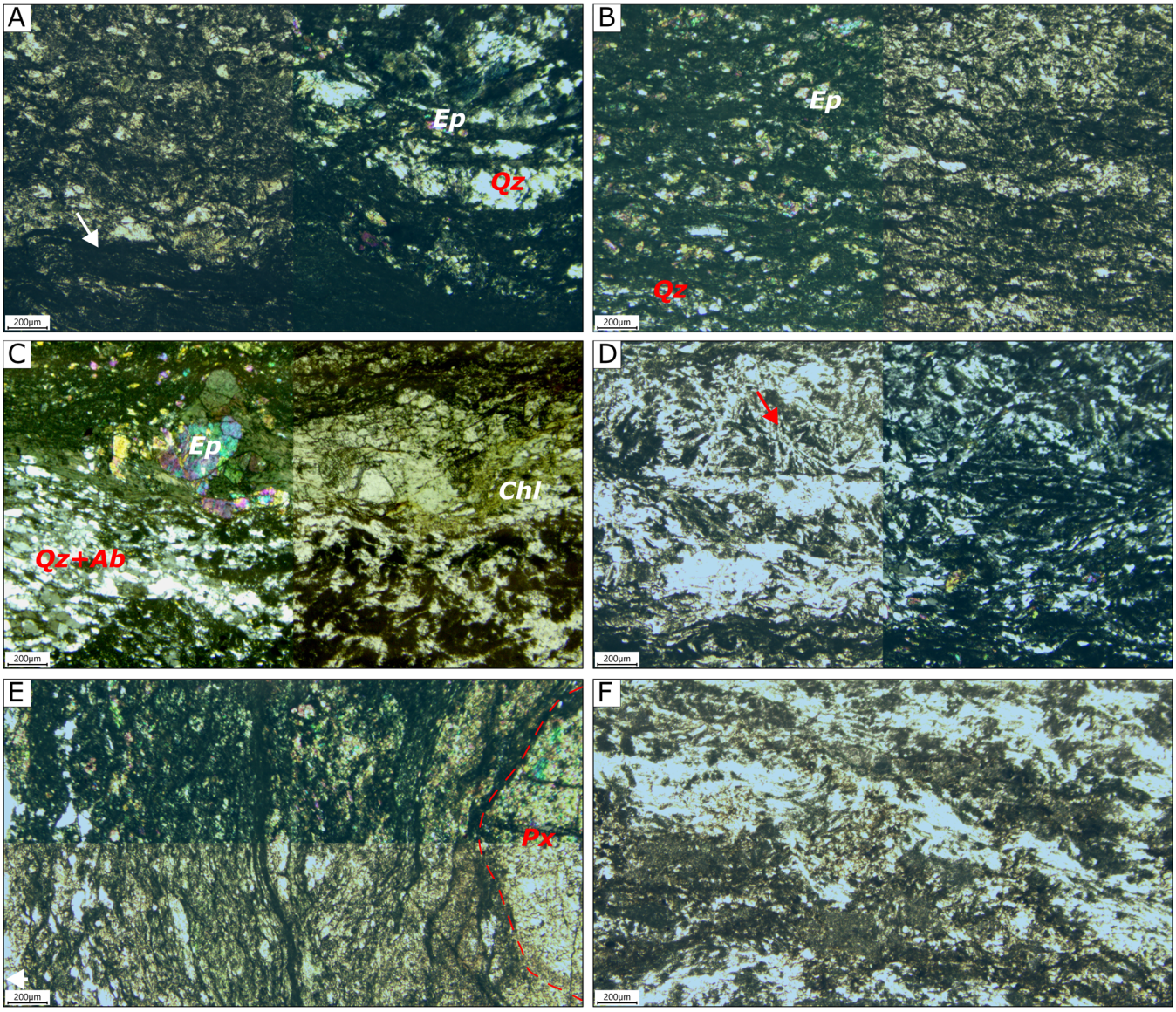

Figure 6. Thin-section photomicrographs of Lithofacies C. (**A**) Textural characteristics of the dark green laminae, consisting of a very fine-grained, dark brown chlorite groundmass (white arrow), embedding aggregates of epidote (Ep) and quartz (Qz). Plane (**left**) and crossed (**right**) polarized light. (**B**) Bright, dark green lamina with larger amounts of epidote porphyroblasts. Plane (**right**) and crossed (**left**) polarized light. (**C**) Quartz–albite-dominated band (Qz-Ab) alternated with chlorite-dominated laminae (Chl) with porphyroblasts of epidote (Ep). On top, a fine-grained lamina with small epidote porphyroblasts occurs. Plane (**right**) and crossed (**left**) polarized light. (**D**) Variolithic texture characterizing the whitish, porous laminae. Arrows indicate albite needles. Plane (**left**) and crossed (**right**) polarized light. (**E**) Concentric arrangement of fine-grained groundmass around totally metamorphosed pyroxene (Px in dashed line) that characterizes the reddish fragments intercalated within the foliation. The white arrow points to the top of the thin section. Plane (**bottom**) and crossed (**top**) polarized light. (**F**) Plane polarized light microphotograph showing dark areas mainly constituted of fine-grained microcrystalline calcite into a quartz–albite-dominated laminae.

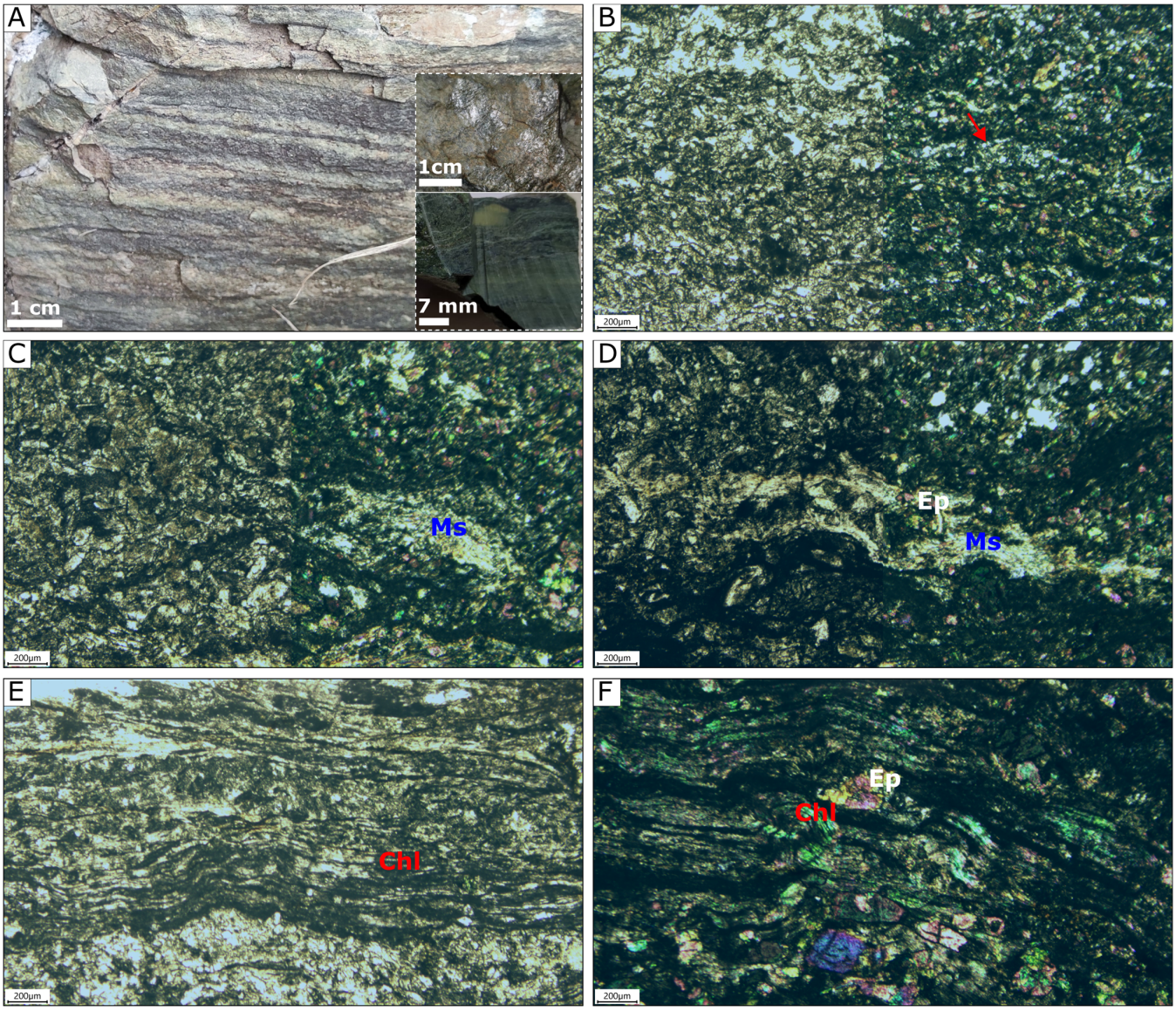

Figure 7. Lithofacies D. (**A**) Field appearance of Lithofacies D, featuring intense green colors and a well-developed foliation, wrapping a whitish clast (lower close-up view), and a silvery luster appearance (upper close-up view). (**B**) Thin-section microphotograph showing fine-grained, mafic-dominated groundmass (epidote and chlorite) and lens-shaped, quartz-dominated regions (red arrow). Plane (**left**) and crossed (**right**) polarized light. (**C**) Thin-section microphotograph of a pseudofelty structure made up of muscovite (Ms) permeating the fine-grained groundmass. Plane (**left**) and crossed (**right**) polarized light. (**D**) Thin-section microphotograph of a pseudofelty structure made up of muscovite (Ms) wrapping crystals of epidote (ep). Plane (**left**) and crossed (**right**) polarized light. (**E**) Thin-section microphotograph under plane polarized light of well-developed bands of chlorite (Chl) overlain with a fine-grained lamina mainly composed of quartz and epidote. (**F**) Thin-section microphotograph under crossed polarized light of well-developed chlorite (Chl) bands wrapping porphyroblasts and trains of epidote (Ep).

4.5. Lithofacies E

Lithofacies E occurs only in the uppermost part of the studied succession with a maximum thickness of more than 350 cm (Figure 2F). It consists of a compact, fine- to medium-grained rock with a predominant dark green color, exhibiting bluish-black tones and a silvery reflection (Figure 8A). The rock has a bright luster and a soapy feel along the schistosity planes. It is characterized by well-developed foliation at a millimetric scale, with alternating fine-grained dark to light green layers and coarser whitish bands. The

internal layering is generally parallel and slightly wavy, without significant disruption of the bands. A detailed observation reveals millimetric reddish particles typically embedded within the foliation.

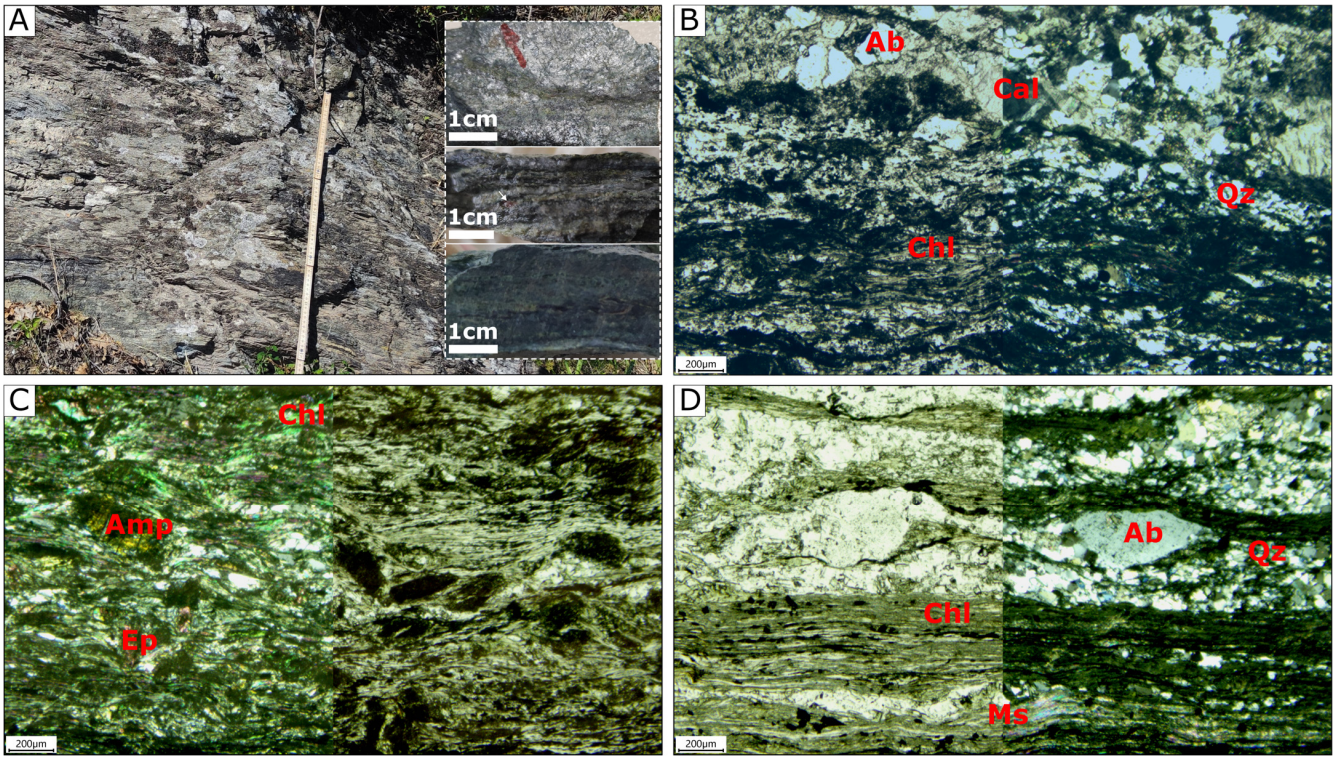

Figure 8. Lithofacies E. (**A**) Field image of Lithofacies E forming tabular levels. Note the predominant dark green color with bluish-black tones characterizing the internal laminae (lower close-up view). Foliation is well developed and composed of a vertical alternation of millimetric-scale dark to light to white bands (middle close-up view), often embedding dispersed reddish particles (white arrow). Schistosity plains often show a bright luster (upper close-up view). (**B**) Thin-section microphotograph showing an alternation of fine-grained, chlorite-dominated laminae (Chl) and quartz-dominated laminae (Qz). On top, the sequence is overlain by a coarser lamina composed of calcite (Cal) embedding porphyroclasts of quartz and albite (Ab). Plane (**left**) and crossed (**right**) polarized light. (**C**) Thin-section microphotograph of well-developed chlorite-dominated laminae (Chl) wrapping mainly porphyroblasts of epidote (Ep) and putative amphibole (Amp). (**D**) Thin-section microphotograph showing alternation of muscovite- (Ms), chlorite- (Chl), and quartz-dominated (Qz) laminae. Note the presence of two porphyroclasts of albite (Ab) wrapped within them.

Thin section observations reveal vertical repetition of chlorite-dominated and quartz-to-calcite-dominated bands, aligned along the foliation, corresponding, respectively, to the dark/light green and whitish layers in mesoscale observations (Figure 8B). Wrapped in the chlorite-dominated bands are generally recognizable porphyroblasts of epidote and rare, putative amphiboles, whereas albite is occasionally recognized as porphyroblasts in the quartz- and calcite-dominated bands (Figure 8C). Occasionally, laminae that are predominantly composed of muscovite occur, including fine-grained porphyroclasts of albite and minor epidote (Figure 8D).

The combination of macroscale observations, microscale textures, and mineralogical composition suggests that beds of Lithofacies E consist of volcaniclastic deposits with larger amounts of particles with non-volcanic origins (volcanic epiclastic deposits, sensu [49]).

5. Discussion

5.1. Protoliths of the Gimigliano Metabasites and Their Emplacement Mechanisms

The identification of protoliths from metaeffusive and metaexplosive rocks can be extremely challenging when they share a common magmatic source and experience the same metamorphic phases, because effusive and explosive products from the same magma would share the same minero-chemical characteristics and then be involved in metamorphic transformations. Oceanic seafloor sequences are rich in basaltic lava flows, different in morphology [50], and are associated with variable amounts of hyaloclastic deposits. These deposits are generated by the interactions between rising lava and seawater [3,51] and are normally emplaced by a wide plethora of processes that generate and transport particles whose dimensions encompass the entire spectrum of particle grainsize [52,53]. Beyond those deposits, pyroclastic deposits generated by explosive activity of basaltic magma mixed with seawater are also frequently documented [1,4–6].

The low metamorphic grade at which Gimigliano metabasites underwent metamorphism totally or partially preserved the stratigraphic features of the rocks and the microscopic relationships existing between the minerals and groundmass [14,15,27,54]. Consequently, it can be considered that the macroscopic characteristics and metamorphic textures observed under the microscope mimic the original volcanic and volcanogenic features, giving us clues for the identification of the protoliths and related emplacement mechanisms [27,55] (Figure 9). A first gross distinction should be made considering what appears to be purely effusive from what appears to be purely sedimentary as protoliths.

The rocks of Lithofacies B, for example, represent the best candidate to be considered metabasalts. Their lepido-nematoblastic texture, characterized by crystals of epidote, hornblende, and minor plagioclase wrapped around by the foliation, easily recalls the porphyritic textures of basalts, in which pyroxene minerals are dispersed in a vitric groundmass that underwent devitrification before the metamorphic process. Their mesoscale appearance as planar layers, without any recognizable pillow-like structures or vitric hyaloclastite surrounding them, indicates that the emplacement of such basalts occurred as lobate or sheet basalts (e.g., [50,51,56]).

In turn, the rocks of Lithofacies A, composed of well-defined, fine-grained bands of alternating mafic and felsic mineralogical assemblages derive from fine-grained protoliths that somehow presented such original stratigraphy and compositional heterogeneity. Distinct elements with different shape and composition, arranged in bands, recall the arrangements of hyaloclastic and/or pyroclastic particles in mid-oceanic ridges [4,52,57]. Hyaloclastic particles are normally sand-sized and generally described as thin, plate-like sideromelane fragments (limu O'Pelè [52]) and angular, polyhedral sideromelane shards, whereas pyroclastic particles include lava fragments (fresh to highly altered), highly vesicular to scoriaceous glassy clasts, and scoria-like fragments [4,7]. All of these particles are normally arranged in well-stratified mm to cm scale volcaniclastic deposits that can be up to hundreds of meters thick [7], therefore, mimicking the strongly foliated layers of Lithofacies A of the Gimigliano metabasites. Generated through explosive eruptions, the volcaniclastic layers were mainly emplaced by the settling of suspended particles from the water column, with minor contributions by density currents [7,58]. Alternatively, volcaniclastic layers could have been accumulated from fallout deposits dispersed by thermal seawater plumes generated by erupting lava [53]. In both cases, Lithofacies A could represent volcaniclastic deposits, settled down from suspended particles, in which mafic bands originally represented portions enriched with denser particles (e.g., lithics and heavy minerals such as pyroxene and amphiboles), whereas felsic bands were enriched with lighter particles (glassy particles) (e.g., [1,5,52]). Similarly, the increase in felsic mineralogical assemblage and muscovite concentration in Lithofacies E in the uppermost part of the investigated

sequence is indicative of a constant increase in non-volcanic (possibly pelagic) particles in the sedimentary budget, as muscovite derives from the metamorphism of clay minerals.

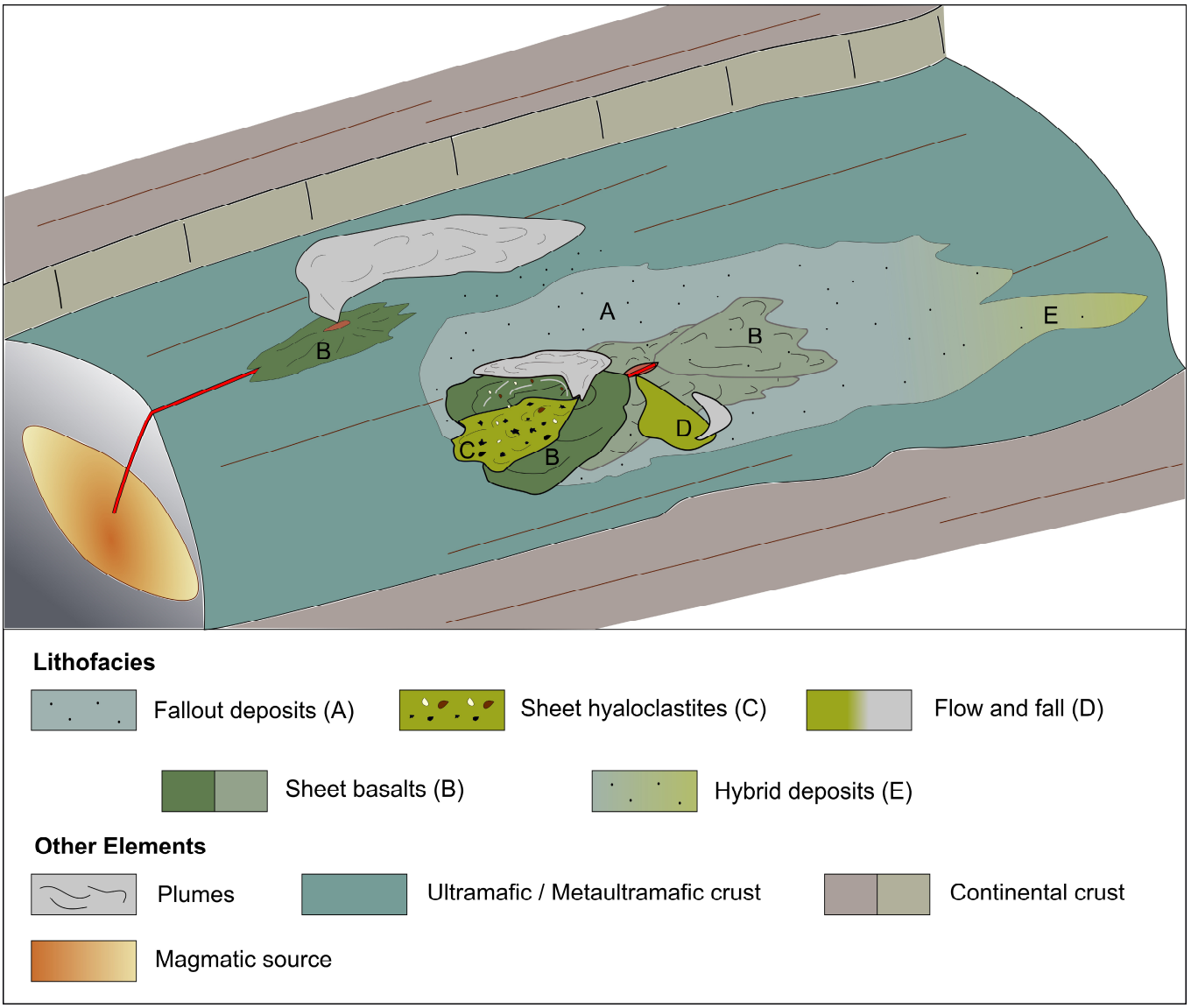

Figure 9. Sketch of the main emplacement mechanisms of the Gimigliano metabasite according to the stratigraphic and petrographic data, within a mid-oceanic ridge framework. Letters refer to lithofacies codes.

In between these two end-members, emplacement mechanisms driven by different grades of interactions among uprising magma, seawater, and exsolved volatiles result in the generation of more complex stratigraphic features and microtextures [53]. Variolitic textures, recognized in whitish discontinuous bands and small particles of Lithofacies C, for example, are commonly described as typical microtextures in hyaloclastic and metahyaloclastic deposits, derived from the quenching processes of extruding lava in contact with water during the formation of hyaloclastic particles [53,59]. Small amounts of elements characterized by an irregular shape represent marly rip-up clasts entertained by uprising magma as peperite-like particles, similar to those observed by [60] in the hyaloclastic deposits of Mt. Etna. Reddish to brown fragments preserve the internal microstructures and pseudo-soft-state, plastically reshaped borders typical of scoriaceous products ejected and accumulated at very high temperatures [52]. In light of this, pseudofelty structures

in Lithofacies D may recall metamorphosed products of sintering processes typical of pyroclastic particles in submarine environments (e.g., [61,62]). Fragments characterized by variable mineralogical assemblages are directly derived from the metamorphism of coarse-grained scoria-like fragments with slightly different mineralogical and geochemical composition (e.g., [7,52]). In view of these characteristics, the described layers could be considered as hyaloclastite sheet layers derived from the explosive interaction between lava and water during the emplacement of sheet basalts, emplaced by density currents on top of basaltic flows [52].

5.2. Reassessing Volcano–Sedimentary Processes in the Calabrian Tethys

The comparison of the Gimigliano metavolcano–sedimentary succession—for many years interpreted only as being composed of metamorphic basalts—with the other metavolcano–sedimentary successions of the Calabrian ophiolites [14,15,30] opens up a new interpretation of the magmatic processes leading to the evolution of this branch of the Western Tethys, helping us to understand the geodynamic significance of the Calabrian branch.

The identification of lobate/sheet basalt layers at Gimigliano draws on differences from the observations reported at Diamante, Fuscaldo–Rose, and Malvito–S. Agata di Esaro successions, where metabasalts are characterized by well-preserved pillow morphologies, rather than sheet-like morphologies [14,30,54]. This difference creates constraints in retrieving the effusive rates that drove the emplacement of basalts along this branch of the Western Tethys. The experiments proposed by [63] demonstrate that lobate to sheet basalts normally require higher flow rates, greater slopes, and lower cooling rates compared to pillow basalts. Observations of modern submarine volcanic terrains also indicate that sheet basalts derive from fissure-type eruptions of fluid lava, whereas pillow basalts result from less voluminous flows, higher in viscosity ([50] and ref. therein). The same observations document that both typologies of basalts can coexist along the same mid-oceanic ridge branch as a consequence of different magma supply along the same ridge [64]. According to [9], higher proportions of sheet basalts in a single ridge segment could also be used to identify the central part of the ridge itself. Therefore, the absence of pillow basalts in the Gimigliano area could be a solid constraint in the reconstruction of the ridge geometry, considering Gimigliano as somehow being located in the central part of the Calabrian ridge segments (or in the central part of a segment within the Calabrian branch of the Western Tethys), whereas the other sectors were located at the offshoots of the same ridge/ridges. Differences in effusive rates were also at the base of the different aspects of hyaloclastite deposits along the Calabrian metaophiolitic successions [14,15,30]. Hyaloclastites are almost fine-grained in Gimigliano, whereas they are described as hyaloclastite breccias on top of the pillow basalts further to the north. The couplings of fine-grained hyaloclastite-sheet basalts and brecciated hyaloclastite-pillow basalts—also documented in other Tethyan successions (e.g., [13,65])—indicate that submarine effusive rates even controlled the generation of hyaloclastite deposits, with high effusive rates inducing the accumulation of sheet basalts and hyaloclastite sheets by explosive interactions between lava and water [52,53], and low effusive rates allowing the disruption of pillow lavas into hyaloclastite breccias during their outcoming (e.g., [51]). High eruptive rates also drove the generation of volcaniclastic deposits [5,53]; therefore, the occurrence of metavolcaniclastic layers in the Gimigliano succession enhances the hypothesis through which the Gimigliano area was a high-effusive branch of the Calabrian oceanic ridge, proximal to eruptive fissures [7].

These stratigraphic characteristics, together with the widespread presence of the ultramafic terranes of the Liguride Complex at the bottom of the volcano–sedimentary succession, would envisage the Calabrian Tethys as being similar to the Gakkel Ridge (Arctic) [1], in which eruptive fissures able to build up flat volcanic edifices distributed

primary volcaniclastic deposits derived from effusive and explosive events onto an oceanic crust (Figure 9). Finding a modern counterpart to the Tethyan branches would be a good opportunity to better constrain the geodynamic setting in which the Mesozoic Ocean formed. The Gakkel Ridge, for example, shares effusive–explosive mechanisms with the Gimigliano area, and it is an ultra-slow spreading ridge, therefore, with a geodynamic configuration similar to that hypothesized for the Tethys in other areas of the world (e.g., [10,65,66]).

6. Conclusions

This multidisciplinary and multiscale study of the metabasite succession within the Gimigliano–Monte-Reventino metaophiolite Unit allowed the characterization of volcano–sedimentary protoliths and the processes responsible for their emplacement. Five lithofacies (A–E) have been recognized, with each reflecting distinct eruptive and depositional processes that that drove the emplacement of the entire metabasite succession. Lithofacies A is characterized by fallout deposits that settled through the water column, while Lithofacies B comprises sheet-like basalt flows. Lithofacies C, composed of hyaloclastite particles, records the direct interaction between lava and seawater, leading to fragmentation and the accumulation of hyaloclastic material. Lithofacies D reflects alternating flow and fallout events, whereas Lithofacies E displays hybrid characteristics, derived from the mixing between volcaniclastic particles and pelagic contributions. The occurrence of sheet basalts suggests volcanological processes dominated by high effusive rates, and the occurrence of primary volcaniclastic deposits indicates that explosive processes also played an important role in building the Gimigliano volcano–sedimentary archive. The comparison of this archive with the other volcano–sedimentary successions along the Calabrian metaophiolites and modern counterparts suggests that the Gimigliano area was potentially the nearest area to a ridge system dominated by spatially variable rates of ascending magma. Such magmatological configuration, next to the widespread presence of metaultramafic rocks at the bottom of the metabasites, would define the Calabrian branch of the Tethys as a slow-spreading oceanic ridge, in line with other Tethyan contexts. Concluding, the present study has demonstrated the importance of a multidisciplinary and multiscale approach in the identification of volcano–sedimentary processes, even though applied to metamorphic successions, as volcano–sedimentary deposits are a repository of crucial information for deciphering past environmental and geodynamic settings and unravelling the complexities of ancient volcanic systems.

Author Contributions: Conceptualization, F.B. (Federica Barilaro) and A.D.C.; methodology, F.B. (Federica Barilaro), A.D.C., G.R. and G.T.; data curation, F.B. (Federica Barilaro); writing—original draft preparation, F.B. (Federica Barilaro) and A.D.C.; writing—review and editing, F.B. (Federica Barilaro), A.D.C., G.C. (Giuseppe Cianflone), G.T., G.R., F.B. (Fabrizio Brutto), R.D., G.C. (Giuseppe Ciccone), A.F. and V.F.; supervision, R.D.; project administration, R.D.; funding acquisition, R.D. All authors have read and agreed to the published version of the manuscript.

Funding: This research has been supported by the funds of the CARG—Project—Geological Map of Italy 1:50,000, within the framework of the DiBEST–ISPRA Agreement (01/12/2022) for the completion of the official Geological Map of Italy, Geological Sheet No. 575 "Catanzaro"-CUP H23C22001040007.

Data Availability Statement: The original contributions presented in this study are included in the article. Further inquiries can be directed to the corresponding authors.

Acknowledgments: The authors wish to express their sincere gratitude to the four anonymous reviewers for their constructive comments and insightful suggestions, which greatly contributed to improving the quality and clarity of the manuscript. The authors warmly thank Gino Romagnoli (ISPRA) for his invaluable guidance and kind support throughout the CARG Project. Sincere appreciation is also extended to Tiziana La Pietra,. Giovanna Chiodo, Salvatore Siviglia, and Domenico Pallaria (Regione Calabria) for their support and effective project management. Vincenzo Festa also acknowledges funds of the PNRR project entitled "*Abrupt Lithofacies Variations IN the stratigraphic record: proxies for environmental and climate changes—ALVIN*." Project Code: 2022APF9M2. CUP: Geo.Prin2022Tropeano.

Conflicts of Interest: The authors declare no conflicts of interest.

Abbreviations

The following abbreviations are used in this manuscript:

MDPI	Multidisciplinary Digital Publishing Institute
DOAJ	Directory of open access journals
TLA	Three letter acronym
LD	Linear dichroism

References

1. Pointbriand, C.W.; Soule, S.A.; Sohn, R.A.; Humphris, S.E.; Kunz, C.; Singh, H.; Nakamura, H.-I.; Jakobsson, M.; Shank, T. Effusive and explosive volcanism on the ultraslow-spreading Gakkel Ridge, 85°E. *Geochem. Geophys. Geosyst.* **2012**, *13*, 10005. [CrossRef]
2. Rubin, K.H.; Soule, S.A.; Chadwick, W.W., Jr.; Fornari, D.J.; Clague, D.A.; Embley, R.W.; Baker, E.T.; Perfit, M.R.; Caress, D.W.; Dziak, R.P. Volcanic eruptions in the deep sea. *Oceanography* **2012**, *25*, 142–157. [CrossRef]
3. White, J.D.L.; Houghton, B.F. Primary volcaniclastic rocks. *Geology* **2006**, *34*, 677–680. [CrossRef]
4. Hekinian, R.; Pineau, F.; Shilobreeva, S.; Bideau, D.; Gracia, E.; Javoy, M. Deep sea explosive activity on the Mid-Atlantic Ridge near 34°50′N: Magma composition, vesicularity and volatile content. *J. Volcanol. Geotherm. Res.* **2000**, *98*, 49–77. [CrossRef]
5. Clague, D.A.; Davis, A.; Dixon, J. Submarine strombolian eruptions on the Gorda Mid-Ocean Ridge. In *Explosive Subaqueous Volcanism*; White, J.D.L., Smellie, J., Clague, D., Eds.; AGU Geophysical Monograph: Washington, DC, USA, 2003; Volume 140, pp. 111–128.
6. Clague, D.A.; Paduan, J.B.; Davis, A.S. Widespread strombolian eruptions of mid-ocean ridge basalt. *J. Volcanol. Geotherm. Res.* **2009**, *180*, 171–188. [CrossRef]
7. Eissen, J.P.; Fouquet, Y.; Hardy, D.; Ondréas, H. Recent MORB volcaniclastic explosive deposits formed between 500 and 1750 m.b.s.l. on the axis of the Mid-Atlantic Ridge, south of the Azores. In *Explosive Subaqueous Volcanism, Geophysical Monograph Series*; White, J.D.L., Smellie, J.L., Clague, D.A., Eds.; AGU: Washington, DC, USA, 2003; Volume 140, pp. 143–166. [CrossRef]
8. Cannat, M. How thick is the magmatic crust at slow spreading oceanic ridges? *J. Geophys. Res.* **1996**, *101*, 2847–2857. [CrossRef]
9. Soule, S.A. Mid-Ocean Ridge Volcanism. In *The Encyclopedia of Volcanoes*, 2nd ed.; Sigurdsson, H., Ed.; Elsevier: Amsterdam, The Netherlands, 2015; p. 1393.
10. Bortolotti, V.; Principi, G. Tethyan ophiolites and Pangea break-up. *Island Arc* **2004**, *14*, 442–470. [CrossRef]
11. Kumar, A.; Sheth, H.; Barman, P.; Ibrahim, M. Volcanic facies as a guide to the palaeodepth and palaeotectonic setting of ancient oceanic crust: The case of the Nidar ophiolite, Ladakh, Indian Trans-Himalaya. *Bull. Volcanol.* **2021**, *83*, 1–14. [CrossRef]
12. Bortolotti, V.; Marroni, M.; Pandolfi, L.; Principi, G.; Saccani, E. Interaction between Mid-Ocean Ridge and Subduction Magmatism in Albanian Ophiolites. *J. Geol.* **2002**, *110*, 561–576. [CrossRef]
13. Tartarotti, P.; Martin, S.; Festa, A.; Balestro, G. Metasediments Covering Ophiolites in the HP Internal Belt of the Western Alps: Review of Tectono-Stratigraphic Successions and Constraints for the Alpine Evolution. *Minerals* **2021**, *11*, 411. [CrossRef]
14. Amodio-Morelli, L.; Bonardi, G.; Colonna, V.; Dietrich, D.; Giunta, G.; Ippolito, F.; Liguori, V.; Lorenzoni, S.; Paglionico, A.; Perrone, V.; et al. L'arco calabro-peloritano nell'orogene appennino-maghrebide. *Mem. Soc. Geol. It.* **1976**, *17*, 1–60.
15. Liberi, F.; Morten, L.; Piluso, E. Geodynamic significance of ophiolites within the Calabrian Arc. *Island Arc* **2006**, *15*, 26–43. [CrossRef]
16. Visalli, R.; Punturo, R.; Cirrincione, R. Petrophysical properties of serpentinite from Calabria. *Minerals* **2023**, *13*, 1132.
17. Apollaro, C.; Marini, L.; Critelli, T.; Barca, D.; Bloise, A.; De Rosa, R.; Liberi, F.; Miriello, D. Investigation of rock-to-water release and fate of major, minor, and trace elements in the metabasalt–serpentinite shallow aquifer of Mt. Reventino (CZ, Italy) by reaction path modelling. *Appl. Geochem.* **2011**, *26*, 1722–1740. [CrossRef]

18. Bonardi, G.; Cavazza, W.; Perrone, V.; Rossi, S. Calabria–Peloritani terrane and northern Ionian Sea. In *Anatomy of an Orogen: The Apennines and Adjacent Mediterranean Basins*; Springer: Dordrecht, The Netherlands, 2001; pp. 287–306.
19. Cirrincione, R.; Fazio, E.; Fiannacca, P.; Ortolano, G.; Pezzino, A.; Punturo, R. The Calabria-Peloritani Orogen, a composite terrane in Central Mediterranean; its overall architecture and geodynamic significance for a pre-Alpine scenario around the Tethyan basin. *Period. di Mineral.* **2015**, *84*, 701–749. [CrossRef]
20. Cirrincione, R.; Fazio, E.; Fiannacca, P.; Ortolano, G.; Pezzino, A.; Punturo, R.; Romano, V.; Sacco, V. The Alpine evolution of the Aspromonte Massif: Constraints for geodynamic reconstruction of the Calabria-Peloritani Orogen. *Geol. Field Trips* **2013**, *5*, 73. [CrossRef]
21. Festa, V.; Cicala, M.; Tursi, F. The Curinga–Girifalco Line in the Framework of the Tectonic Evolution of the Remnant Alpine Chain in Calabria (Southern Italy). *Int. J. Earth Sci.* **2020**, *109*, 2583–2598. [CrossRef]
22. Tursi, F.; Spiess, R.; Festa, V.; Fregola, R.A. Hercynian Subduction-Related Processes within the Metamorphic Continental Crust in Calabria (Southern Italy). *J. Metamorph. Geol.* **2020**, *38*, 771–793. [CrossRef]
23. Tursi, F.; Acquafredda, P.; Festa, V.; Fornelli, A.; Langone, A.; Micheletti, F.; Spiess, R. What Can High-P Sheared Orthogneisses Tell Us? An Example from the Curinga–Girifalco Line (Calabria, Southern Italy). *J. Metamorph. Geol.* **2021**, *39*, 919–944. [CrossRef]
24. De Roever, E.W.F. Lawsonite-albite facies metamorphism near Fuscaldo, Calabria (southern Italy), its geological significance and petrological aspects. *GUA Pap. Geol.* **1972**, *1*, 1–171.
25. Dietrich, D.; Scandone, P. The position of the basic and ultrabasic rocks in the tectonic units of the Southern Apennines. *Atti Accad. Pontaniana* **1972**, *21*, 61–75.
26. Ogniben, L. Schema Geologico della Calabria in base ai dati odierni. *Geol. Romana* **1973**, *12*, 243–585.
27. Beccaluva, L.; Macciotta, G.; Spadea, P. Petrology and geodynamic significance of the Calabria-Lucania ophiolites. *Rend. Soc. Ital. Mineral. Petrol.* **1982**, *38*, 973–987.
28. Guerrera, F.; Martín-Algarra, A.; Perrone, V. Late Oligocene-Miocene syn-late-orogenic successions in Western and Central Mediterranean Chains from the Betic Cordillera to the Southern Apennines. *Terra Nova* **1993**, *5*, 525–544. [CrossRef]
29. Cello, G.; Invernizzi, C.; Mazzoli, S. Structural signature of tectonic processes in the Calabrian Arc, southern Italy: Evidence from the oceanic-derived Diamante-Terranova Unit. *Tectonics* **1996**, *15*, 187–200. [CrossRef]
30. Liberi, F.; Piluso, E. Tectonometamorphic evolution of the ophiolitic sequences from Northern Calabrian Arc. *Ital. J. Geosci.* **2009**, *128*, 483–493.
31. Tortorici, L. Lineamenti geologico-strutturali dell'Arco Calabro Peloritano. *Rend. Soc. Ital. Mineral. Petrol.* **1982**, *4*, 927–940.
32. Ogniben, L. Schema introduttivo alla geologia del confine calabro-lucano. *Mem. Soc. Geol. It.* **1969**, *8*, 453–763.
33. Scandone, P. Structure and evolution of the Calabrian Arc. *Earth Evol. Sci.* **1982**, *3*, 172–180.
34. Morten, L.; Tortorici, L. Geological framework of the ophiolite-bearing allochtonous terranes of the Calabrian Arc and Lucanian Apennine. In *Italian Eclogites and Related Rocks*; Morten, L., Ed.; Accademia Nazionale delle Scienze detta dei XL: Roma, Italy, 1993; Volume 13, pp. 145–150.
35. Piluso, E.; Cirrincione, R.; Morten, L. Ophiolites of the Calabrian Peloritani Arc and their relationships with the Crystalline Basement (Catena Costiera and Sila Piccola, Calabria, Southern Italy). *Ofioliti* **2000**, *25*, 117–140.
36. Messina, A.; Russo, S.; Borghi, A.; Colonna, V.; Compagnoni, R.; Caggianelli, A.; Fornelli, A.; Piccarreta, G. Il Massiccio della Sila Settore settentrionale dell'Arco Calabro-Peloritano. *Boll. Soc. Geol. It.* **1994**, *113*, 359–586.
37. Piccarreta, G.; Zirpoli, G. Le Rocce Verdi del Monte Reventino. *Boll. Soc. Geol. It.* **1969**, *88*, 469–488.
38. Punturo, R.; Fiannacca, P.; Lo Giudice, A.; Pezzino, A.; Cirrincione, R.; Liberi, F.; Piluso, E. Le cave storiche della "pietra verde" di Gimigliano e Monte Reventino (Calabria): Studio petrografico e geochimico. *Boll. Soc. Gioenia Sci. Nat.* **2004**, *37*, 37–59.
39. Punturo, R.; Visalli, R.; Cirrincione, R. A Review of the Mineralogy, Petrography, and Geochemistry of Serpentinite from Calabria Regions (Southern Italy): Problem or Georesource? *Minerals* **2023**, *13*, 1132. [CrossRef]
40. Lanzafame, G.; Zuffa, G.G. Geologia e Petrografia del Foglio Bisignano (Bacino del Crati, Calabria). *Geol. Romana* **1976**, *15*, 223–270.
41. Spadea, P.; Tortorici, L.; Lanzafame, G. Serie ofiolitifere fra Tarsia e Spezzano Albanese (Calabria): Stratigrafia, petrografia, rapporti strutturali. *Mem. Soc. Geol. It.* **1976**, *17*, 135–174.
42. Punturo, R.; Mine, S.; Motra, H.B.; Lanzafame, G.; Indelicato, V.; Pappalardo, G.; Cirrincione, R. Greenstone of Calabria: A multi-analytical characterization of heritage metabasite from Southern Italy. *Case Stud. Constr. Mater.* **2024**, *20*, e03269. [CrossRef]
43. Lanzafame, G.; Spadea, P.; Tortorici, L. Mesozoic ophiolites of northern Calabria and Lucanian Apennines (Southern Italy). *Ofioliti* **1979**, *4*, 173–182.
44. Colonna, V.; Piccarreta, G. Schema strutturale della Sila Piccola Meridionale. *Boll. Soc. Geol. It.* **1975**, *94*, 1975.
45. Rossetti, F.; Faccenna, C.; Goffé, B.; Funiciello, R.; Monié, P. Tectono-metamorphic evolution of the ophiolite-bearing HP/LT Gimigliano-Monte Reventino Unit (Gimigliano, Sila Piccola); insights for the tectonic evolution of the Calabrian Arc. *Ital. J. Geosci.* **2002**, *121*, 51–67.

46. Colonna, V.; Zanettin Lorenzoni, E. Gli scisti cristallini della Sila Piccola. 2°: Rapporti tra la formazione delle filladi e la formazione delle pietre verdi nella zona di Gimigliano. *Mem. Soc. Geol. It.* **1972**, *11*, 261–292.
47. Vai, G.B. Il segmento Calabro-Peloritano dell'orogene Ercinicio Disaggregazione palinspastica. *Boll. Soc. Geol. It.* **1992**, *111*, 109–129.
48. Whitney, D.L.; Evans, B.W. Abbreviations for Names of Rock-Forming Minerals. *Am. Miner.* **2010**, *95*, 185–187. [CrossRef]
49. Di Capua, A.; De Rosa, R.; Kereszturi, G.; Le Pera, E.; Rosi, M.; Watt, S.F. Volcanically-derived deposits and sequences: A unified terminological scheme for application in modern and ancient environments. In *Volcanic Processes in the Sedimentary Record: When Volcanoes Meet the Environment*; Geological Society: London, UK, 2023; Volume 520, pp. 11–27.
50. Kennish, M.J.; Lutz, R.A. Morphology and distribution of lava flows on mid-ocean ridges: A review. *Earth-Sci. Rev.* **1998**, *43*, 63–90. [CrossRef]
51. White, J.D.L.; McPhie, J.; Soule, S.A. Submarine Lavas and Hyaloclastite. In *The Encyclopedia of Volcanoes*, 2nd ed.; Sigurdsson, H., Ed.; Elsevier: Amsterdam, The Netherlands, 2015; p. 1393.
52. Maicher, D.; White, J.D.L.; Batiza, R. Sheet hyaloclastite: Density-current deposits of quench and bubble-burst fragments from thin, glassy sheet lava flows, Seamount Six, Eastern Pacific Ocean. *Mar. Geol.* **2000**, *171*, 75–94. [CrossRef]
53. Cas, R.A.F.; Simmons, J.M. Why deep-water eruptions are so different from subaerial eruptions. *Front. Earth Sci.* **2018**, *6*, 00198. [CrossRef]
54. Spadea, P. Contributo alla conoscenza dei metabasalti ofiolitici della Calabria settentrionale e centrale e dell'Appennino Lucano. *Rend. Soc. Ital. Mineral. Petrol.* **1979**, *35*, 251–276.
55. Furnes, H. Meta-hyaloclastite breccias associated with Ordovician pillow javas in the Solund area, west Norway. *Norsk Geol. Tidsskr.* **1972**, *52*, 385–407.
56. Furnes, H.; McLoughlin, N.; Muehlenbachs, K.; Banerjee, N.; Staudigel, H.; Dilek, Y.; de Wit, M.; Van Kranendonk, M.J.; Schiffman, P. Oceanic pillow lavas and hyaloclastites as habitats for microbial life through time–a review. In *Links Between Geological Processes, Microbial Activities and Evolution of Life: Microbes and Geology*; Springer: Berlin/Heidelberg, Germany, 2008; pp. 1–68.
57. Maicher, D.; White, J.D.L. The formation of deep-sea Limu o'Pelé. *Bull. Volcanol.* **2001**, *63*, 482–496. [CrossRef]
58. Carey, S.N.; Schneider, J.-L. Volcaniclastic processes and deposits in the deep-sea. In *Developments in Sedimentology*; Elsevier: Amsterdam, The Netherlands, 2011; Volume 63, pp. 457–515.
59. Ghose, N.C.; Chatterjee, N.; Fareeduddin. Ophiolite around the Indian plate margin. In *A Petrographic Atlas of Ophiolite*; Springer: New Delhi, India, 2014; pp. 9–24. [CrossRef]
60. Corsaro, R.A.; Mazzoleni, P. Textural evidence of peperites inside pillow lavas at Acicastello Castle Rock (Mt. Etna, Sicily). *J. Volcanol. Geotherm. Res.* **2002**, *114*, 219–229. [CrossRef]
61. Di Capua, A.; Groppelli, G. Emplacement of pyroclastic density currents (PDCs) in a deep-sea environment: The Val d'Aveto Formation case (Northern Apennines, Italy). *J. Volcanol. Geotherm. Res.* **2016**, *328*, 1–8. [CrossRef]
62. Di Capua, A.; Barilaro, F.; Szepesi, J.; Lukács, R.; Gál, P.; Norini, G.; Sulpizio, R.; Soós, I.; Harangi, S.; Groppelli, G. Correlating volcanic dynamics and the construction of a submarine volcanogenic apron: An example from the Badenian (Middle Miocene) of North-Eastern Hungary. *Mar. Pet. Geol.* **2021**, *126*, 104944. [CrossRef]
63. Gregg, T.K.P.; Fink, J.H. Quantification of submarine lava-flow morphology through analog experiments. *Geology* **1995**, *23*, 73–76. [CrossRef]
64. Colman, A.; Sinton, J.M.; White, S.M.; McClinton, J.T.; Bowles, J.A.; Rubin, K.H.; Behn, M.D.; Cushman, B.; Eason, D.E.; Gregg, T.K.P.; et al. Effects of variable magma supply on mid-ocean ridge eruptions: Constraints from mapped lava flow fields along the Galápagos Spreading Center. *Geochem. Geophys.Geosyst.* **2012**, *13*, 1–28. [CrossRef]
65. De Togni, M.; Gattiglio, M.; Ghignone, S.; Festa, A. Pre-Alpine Tectono-Stratigraphic Reconstruction of the Jurassic Tethys in the High-Pressure Internal Piedmont Zone (Stura di Viù Valley, Western Alps). *Minerals* **2021**, *11*, 361. [CrossRef]
66. Piccardo, G.B.; Padovano, M.; Guarnieri, L. The Ligurian Tethys: Mantle processes and geodynamics. *Earth-Sci. Rev.* **2014**, *138*, 409–434. [CrossRef]

Disclaimer/Publisher's Note: The statements, opinions and data contained in all publications are solely those of the individual author(s) and contributor(s) and not of MDPI and/or the editor(s). MDPI and/or the editor(s) disclaim responsibility for any injury to people or property resulting from any ideas, methods, instructions or products referred to in the content.